

# Multigap Superconductivity in $\text{Y}_2\text{C}_3$ : A $^{13}\text{C}$ -NMR Study

A. HARADA<sup>1\*</sup>, S. AKUTAGAWA<sup>2</sup>, Y. MIYAMICHI<sup>1</sup>, H. MUKUDA<sup>1</sup>, Y. KITAOKA<sup>1</sup> and J. AKIMITSU<sup>2</sup>

<sup>1</sup>*Department of Materials Engineering Science, Graduate School of Engineering Science, Osaka University, Toyonaka, Osaka 560-8531, Japan*

<sup>2</sup>*Department of Physics and Mathematics, Aoyama-Gakuin University, Sagami-hara, Kanagawa 229-8558, Japan*

(Received October 2, 2018)

We report on the superconducting (SC) properties of  $\text{Y}_2\text{C}_3$  with a relatively high transition temperature  $T_c = 15.7\text{ K}$  investigated by  $^{13}\text{C}$  nuclear-magnetic-resonance (NMR) measurements under a magnetic field. The  $^{13}\text{C}$  Knight shift has revealed a significant decrease below  $T_c$ , suggesting a spin-singlet superconductivity. From an analysis of the temperature dependence of the nuclear spin-lattice relaxation rate  $1/T_1$  in the SC state,  $\text{Y}_2\text{C}_3$  is demonstrated to be a multigap superconductor that exhibits a large gap  $2\Delta/k_B T_c = 5$  at the main band and a small gap  $2\Delta/k_B T_c = 2$  at other bands. These results have revealed that  $\text{Y}_2\text{C}_3$  is a unique multigap s-wave superconductor similar to  $\text{MgB}_2$ .

KEYWORDS: lanthanoid carbide, metal, superconductivity, multigap, NMR,  $\text{Y}_2\text{C}_3$

The discovery of superconductivity in  $\text{MgB}_2$ , which exhibits a high superconducting (SC) transition temperature  $T_c \sim 40\text{ K}$ , has attracted much interest.<sup>1</sup> Motivated by this discovery, intensive effort is devoted to the search for a new high- $T_c$  material in a similar system that contains light elements B and C. Meanwhile, Amano *et al.* reported that  $\text{Y}_2\text{C}_3$  prepared under high pressure ( $\sim 5\text{ GPa}$ ) is a superconductor with a relatively high  $T_c \sim 18\text{ K}$ ,<sup>2</sup> although the superconductivity in this compound was already reported to emerge at  $T_c \sim 6\text{--}11\text{ K}$ .<sup>3</sup> As for SC characteristics, the specific heat measurements on the newly synthesized high-purity samples of  $\text{Y}_2\text{C}_3$  have revealed that a gap size of the respective samples with  $T_c = 11.6, 13.6$ , and  $15.2\text{ K}$  increases as  $2\Delta/k_B T_c = 3.6, 4.1$ , and  $4.4$ .<sup>4</sup> This result raises a question why  $T_c$  and  $2\Delta/k_B T_c$  vary significantly depending on sintering conditions. Further systematic experiments are required to gain deep insight into the SC characteristics of this compound.

$\text{Y}_2\text{C}_3$  crystallizes in the cubic  $\text{Pu}_2\text{C}_3$ -type structure (space group  $I43d$ ) without an inversion center, consisting of the dimers of carbon atoms. The SC properties of the sample previously reported by Amano *et al.* did not exhibit a single SC transition as seen in the inset of Fig. 1(a), pointing to a contamination of extrinsic multiple phases.<sup>2</sup> Recently, Akutagawa *et al.* have succeeded in preparing a single phase of  $\text{Y}_2\text{C}_3$ , which enables us to extract intrinsic electronic and SC properties in  $\text{Y}_2\text{C}_3$ . From the specific-heat measurements of this sample, the Sommerfeld coefficient  $\gamma \sim 6.3\text{ mJ/mol}\cdot\text{K}^2$  and Debye temperature  $\theta_D \sim 530\text{ K}$  were estimated for the sample with  $T_c = 15.2\text{ K}$ .<sup>4</sup> This result suggests that its high Debye temperature makes  $T_c$  relatively high despite its small Sommerfeld coefficient. As in  $\text{MgB}_2$ , the light-element constituent like boron and carbon plays a vital role in enhancing  $T_c$  in general. In the SC state, the temperature ( $T$ ) dependence of the specific heat exhibits an exponential decrease with  $2\Delta/k_B T_c = 4.4$  upon cooling well below  $T_c$ , suggesting a strong-coupling isotropic su-

perconductivity. From an other context, it is noteworthy that a novel SC nature for  $\text{CePt}_3\text{Si}$  and  $\text{Li}_2\text{Pt}_3\text{B}$  without inversion symmetry is a recent interesting topic because the admixture of spin-singlet and spin-triplet SC state is shown to emerge due to the spin-orbit coupling.<sup>5,6</sup> Likewise, determining the order-parameter symmetry and a detailed gap structure is an underlying issue in the newly synthesized high-quality  $\text{Y}_2\text{C}_3$  without inversion symmetry.

In this letter, we report on the SC order-parameter symmetry and gap structure of  $\text{Y}_2\text{C}_3$  with a relatively high  $T_c = 15.7\text{ K}$  ( $H = 0$ ) via  $^{13}\text{C}$  nuclear-magnetic-resonance (NMR) measurements under a magnetic field.  $\text{Y}_2\text{C}_3$  was synthesized by arc melting and high pressure.<sup>4</sup> The sample was confirmed to nearly consist of a single phase by X-ray diffraction analyses, with the formation of a primitive  $\text{Pu}_2\text{C}_3$ -type structure. The polycrystalline sample for  $^{13}\text{C}$ -NMR measurement was slightly enriched with  $^{13}\text{C}$  ( $^{12}\text{C} : ^{13}\text{C} = 9 : 1$ ) in order to improve the NMR signal-to-noise ratio.  $T_c = 15.7$  and  $12.2\text{ K}$  were determined by ac-susceptibility measurements at  $H = 0$  and  $9.85\text{ T}$ , respectively. The NMR experiment was performed by the conventional spin-echo method at  $H = 9.85\text{ T}$  in the  $T$  range of  $1.8\text{--}70\text{ K}$ .

Figures 1(a) and 1(b) show the  $^{13}\text{C}$ -NMR spectra of  $\text{Y}_2\text{C}_3$  for the previous sample reported in ref. 2 and the present sample, respectively, in the normal state at  $T = 15\text{ K}$  and  $H = 9.85\text{ T}$ . Note that the spectra for the previous sample are composed of  $^{13}\text{C}$ -NMR signals arising from  $\text{Y}_3\text{C}$ ,  $\text{YC}_2$ , and  $\text{Y}_2\text{C}_3$ , demonstrating the contamination of extrinsic multiphases, whereas the spectra for the present sample consist of a nearly single peak from  $\text{Y}_2\text{C}_3$  with a small contamination of  $\text{YC}_2$ . The NMR intensity for each phase coincides with the x-ray intensity as expected. The full width at half maximum (FWHM) in the  $^{13}\text{C}$ -NMR spectrum of  $\text{Y}_2\text{C}_3$  is as small as  $8\text{ kHz}$ , ensuring good sample quality. Actually, a single SC transition at  $T_c = 15.7\text{ K}$  was corroborated by the susceptibility measurement at  $H = 10\text{ Oe}$  as seen in the inset of Fig. 1(b).

\*E-mail address: aharada@nmr.mp.es.osaka-u.ac.jp

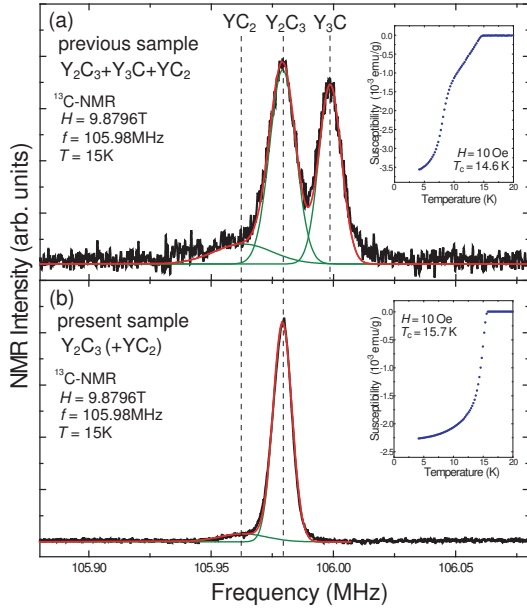


Fig. 1. (Color online)  $^{13}\text{C}$ -NMR spectra of  $\text{Y}_2\text{C}_3$  for (a) the previous sample reported in ref. 2 and (b) the present sample in the normal state at  $T = 15\text{ K}$  and  $H = 9.85\text{ T}$ . Note that the spectra for the previous sample are composed of NMR signals arising from  $\text{Y}_3\text{C}$ ,  $\text{YC}_2$ , and  $\text{Y}_2\text{C}_3$ , demonstrating the contamination of extrinsic multiphases, whereas the spectra for the present sample nearly consist of a single peak from  $\text{Y}_2\text{C}_3$  with a small contamination of  $\text{YC}_2$ . The insets of both figures show the  $T$  dependence of SC diamagnetic susceptibility down to  $4.2\text{ K}$ .

Figure 2(a) shows the  $T$  dependence of  $^{13}\text{C}$  Knight shift (KS) in  $\text{Y}_2\text{C}_3$ , which is determined relative to the resonance frequency of tetramethylsilane (TMS) as a reference substance ( $K[\text{TMS}] \sim 0\text{ ppm}$ ). A clear decrease in KS and an increase in FWHM below  $T_c$  are indicated in Figs. 2(a) and 2(b), which are derived from the  $T$  dependence of NMR spectra as shown in the inset of Fig. 2. In intermediate fields ( $H_{c1} \ll H \ll H_{c2}$ ) where the vortices form a dense lattice, we estimate coherence length and the distance between the vortices to be  $d \sim 160\text{ \AA}$ , and  $\xi \sim 34\text{ \AA}$ , respectively.<sup>8</sup> As a result, a diamagnetic field is led to be  $H_{\text{dia}} \sim -0.3\text{ Oe}$  using the relation  $H_{\text{dia}} = -H_{c1} \ln(\beta e^{-1/2} d/\xi) / \ln \kappa$ ,<sup>7,8</sup> ( $\kappa = \lambda/\xi$ ) and hence a diamagnetic shift is obtained as  $K_{\text{dia}} \sim 3 \times 10^{-4}\%$  at  $H = 9.85\text{ T}$ . Here, we used  $H_{c1} = 3.3\text{ mT}$ ,<sup>4</sup> the London penetration depth  $\lambda = 4470\text{ \AA}$ ,<sup>4</sup>  $\beta = 0.381$  for the case of triangular lattice,<sup>7</sup>  $d \sim 160\text{ \AA}$ , and  $\xi \sim 34\text{ \AA}$ . Thus, the estimated value of  $K_{\text{dia}}$  is one order of magnitude smaller than the decrease in KS observed below  $T_c$ , demonstrating that the decrease in KS is due to the reduction of spin susceptibility associated with the onset of the spin-singlet SC state. If the spin susceptibility was assumed to vanish at low  $T$  due to the formation of spin-singlet Cooper pairing, the orbital and spin part of KS are tentatively estimated to be  $K_{\text{orb}} \sim 0.028\%$  and  $K_s \sim 0.005\%$ , respectively. A possible cause for the increase in FWHM may be due to an inhomogeneous distribution of vortex lattices, which eventually makes either  $d$  or  $\lambda$  distribute. Further systematic NMR measurements at low  $H$  are required for inspecting a structure of vortex lattices.

Next, we deal with the  $T$  dependence of nuclear spin-

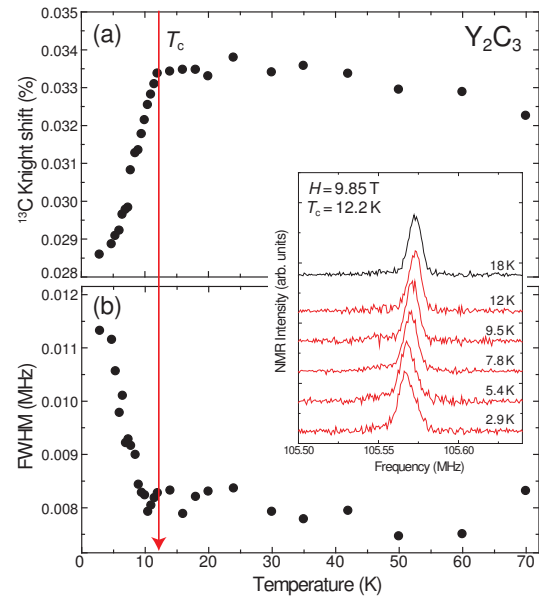


Fig. 2. (Color online)  $T$  dependences of (a)  $^{13}\text{C}$  Knight shift and (b) full width at half maximum (FWHM) of  $^{13}\text{C}$ -NMR spectrum in  $\text{Y}_2\text{C}_3$  at  $H = 9.85\text{ T}$ .  $T_c = 12.2\text{ K}$  is determined by the ac-susceptibility measurement at  $H = 9.85\text{ T}$  as shown by an arrow pointing downward. The inset shows the NMR spectra at  $T = 2.9, 5.4, 7.8, 9.5, 12,$  and  $18\text{ K}$ , respectively.

lattice relaxation rate ( $1/T_1$ ) in order to clarify the gap structure. The  $1/T_1$  for  $^{13}\text{C}$  with nuclear spin  $I = 1/2$  is uniquely determined from a simple exponential recovery curve of nuclear magnetization given by the relation  $[M(\infty) - M(t)]/M(\infty) = \exp(-t/T_1)$ . Here,  $M(t)$  and  $M(\infty)$  are the nuclear magnetizations at a time  $t$  after the saturation pulse and at the thermal equilibrium condition, respectively. Figure 3 presents the  $T$  dependence of  $1/T_1$  at  $H = 9.85\text{ T}$ . In the normal state, the law  $T_1 T = \text{const.}$  is valid down to  $T_c$ . In the SC state,  $1/T_1$  is also precisely measured from a simple exponential recovery curve such as  $[M(\infty) - M(t)]/M(\infty) = \exp(-t/T_1)$ , as seen in the inset of Fig. 4(a). This is because the possible contribution to  $1/T_1$  arising from normal vortex cores is very small, if any, when  $\xi \sim 34\text{ \AA} \ll d \sim 160\text{ \AA}$ .

The inset in Fig. 3 shows  $(T_1 T)_{\text{const.}} / (T_1 T)$  vs  $T/T_c$  for  $\text{Y}_2\text{C}_3$  at  $H = 9.85\text{ T}$  and for  $\text{MgB}_2$  with  $T_c = 29\text{ K}$  at  $H = 4.4\text{ T}$ .<sup>10</sup> Here,  $(T_1 T)_{\text{const.}}$  denotes constant values in normal state. In the SC state, we note that a tiny coherence peak is observed in  $1/T_1$  just below  $T_c$  for  $\text{Y}_2\text{C}_3$  as in  $\text{MgB}_2$ . This is indicative of a full gap opening in  $\text{Y}_2\text{C}_3$  as in  $\text{MgB}_2$ . A reason why the coherence peak is depressed in these compounds may be due to a strong electron-phonon coupling that causes the large life time broadening of quasiparticles induced by thermally excited phonons as reported in ref. 10. In fact, the strong-coupling BCS superconductor such as  $\text{TiMo}_6\text{Se}_{7.5}$  does not show a clear coherence peak.<sup>11</sup> Note that the  $T$  dependence of  $1/T_1$  well below  $T_c$  does not exhibit a simple exponential decrease, but seems to have a kink at around  $T = 5\text{ K}$ . In order to gain further insight into this unique and relevant relaxation behavior with a possible gap structure in the SC state for  $\text{Y}_2\text{C}_3$ , we present in Fig. 4 the Arrhenius plot of  $(T_1 T)/(T_1 T)_{\text{const.}}$  vs  $T_c/T$

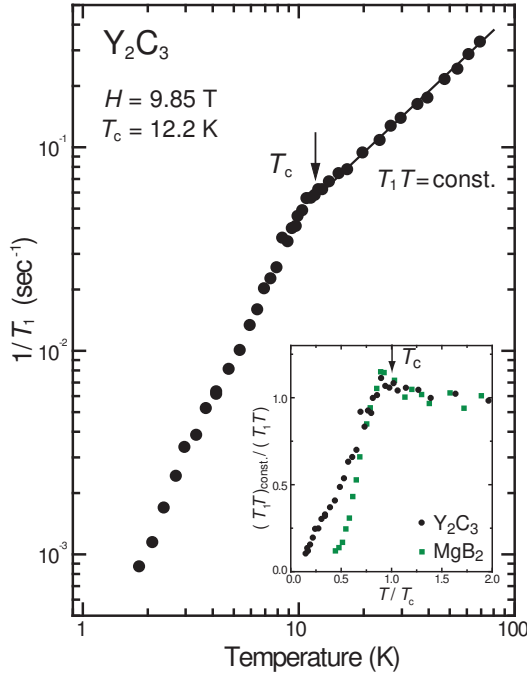


Fig. 3. (Color online)  $T$  dependence of  $1/T_1$  for  $\text{Y}_2\text{C}_3$  with  $T_c = 12.2\text{ K}$  at  $H \sim 9.85\text{ T}$ . A tiny coherence peak just below  $T_c$  is observed for  $\text{Y}_2\text{C}_3$  as in  $\text{MgB}_2$  as shown in the inset. The inset shows the  $(T_1T)_{\text{const.}}/(T_1T)$  vs  $T/T_c$  curve for  $\text{Y}_2\text{C}_3$  (solid circles) at  $H = 9.85\text{ T}$  and for  $\text{MgB}_2$  (solid squares) with  $T_c = 29\text{ K}$  at  $H = 4.4\text{ T}$ .<sup>10</sup> Here,  $(T_1T)_{\text{const.}}$  denotes constant values in normal state.

with  $T_c = 12.2\text{ K}$  at  $H = 9.85\text{ T}$ . It is evident that a power-law behavior in  $1/T_1$  such as  $1/T_1T \propto T^2$  (see the dashed line in the figure) is not valid at all. Instead, when noting that a line in this plot corresponds to an exponential  $T$  dependence in  $1/T_1T$ , it is supposed that a large full gap seemingly opens in a high-temperature regime in the SC state, but low-lying quasiparticle excitations in a low-temperature regime are dominated by the presence of a small full gap. In fact, from respective slopes in this plot in the  $T$  range of  $5\text{ K} - T_c = 12.2\text{ K}$  and at temperatures lower than  $5\text{ K}$ , gap sizes are estimated to be  $2\Delta/k_B T_c \sim 5$  and  $2$ , which suggests that two kinds of SC energy gaps exist, namely, multigap superconductivity takes place in  $\text{Y}_2\text{C}_3$ . We stress that this novel relaxation behavior in the SC state for  $\text{Y}_2\text{C}_3$  is not due to some inhomogeneous effect originating from the presence of vortex cores and/or a distribution of  $T_c$  because  $1/T_1$  is uniquely determined from the simple exponential recovery curve of nuclear magnetization as shown in the inset of Fig. 4.

Here, we apply a phenomenological multigap model for nodeless superconductivity to understand the novel relaxation behavior in the SC state. Figure 5 shows the  $T$  dependence of  $1/T_1T$ . In such a model,  $T_1(T_c)/T_1(T)$  is expressed as

$$\frac{T_1(T_c)}{T_1(T)} = \frac{\alpha^2}{\alpha^2 + \beta^2} \frac{1}{T_1}(\Delta_\alpha) + \frac{\beta^2}{\alpha^2 + \beta^2} \frac{1}{T_1}(\Delta_\beta),$$

where  $\alpha$  and  $\beta$  are defined as the respective fractions of  $N(E_F) \times A_{\text{hf}}$  with SC gap  $\Delta_\alpha$  and  $\Delta_\beta$  and  $\alpha + \beta = 1$ .  $N(E_F)$  and  $A_{\text{hf}}$  are the density of states (DOS) at the

Fermi level and the hyperfine coupling constant, respectively. Here,

$$\frac{1}{T_1}(\Delta) = \frac{2}{k_B T_c} \int_0^\infty dE [N_s^2(E) + M_s^2(E)] f(E) [1 - f(E)],$$

where  $N_s(E)$  is the DOS,  $M_s(E)$  is the anomalous DOS originating from the coherence effect inherent to a spin-singlet SC state and  $f(E)$  is the Fermi distribution function.<sup>12</sup> Note that  $N_s(E)$  and  $M_s(E)$  are averaged over an energy broadening function assuming a rectangle shape with a width  $2\delta$  and a height  $1/2\delta$ .<sup>13</sup> We use  $\delta/\Delta(0) = 0.3$  in the calculation. A theoretical curve based on the multigap model is actually in good agreement with the experiment using  $\beta = 0.75$  and  $2\Delta_\beta/k_B T_c = 5$  for the main band, and  $\alpha = 0.25$  and  $2\Delta_\alpha/k_B T_c = 2$  for other bands as shown by the solid curve in Fig. 5. It is notable that the large gap at the dominant Fermi surface is larger than the weak-coupling BCS value of  $2\Delta/k_B T_c = 3.5$ , indicating a strong electron-phonon coupling and being consistent with the specific-heat result.<sup>4</sup> The present  $^{13}\text{C}$ -NMR has revealed that the superconductivity in  $\text{Y}_2\text{C}_3$  is characterized by a large gap at the main Fermi surface and a small gap at others. This may be consistent with the band calculation which shows the presence of Fermi surfaces consisting of three dimensional multisheets due to the hybridization between Y- $d$  derived states and antibonding C-dimers derived  $p$ -states.<sup>9</sup> We should pay attention to the relationship between the multigap and  $T_c$ . Although  $\text{Y}_2\text{C}_3$  is a superconductor with no inversion symmetry, the present experiments have revealed that this noncentrosymmetric compound is a spin-singlet superconductor with full gaps at all the Fermi surfaces, and hence rules out the possibility of the admixture of spin-triplet order parameter which is the recent underlying topic for the superconductors with no inversion symmetry.

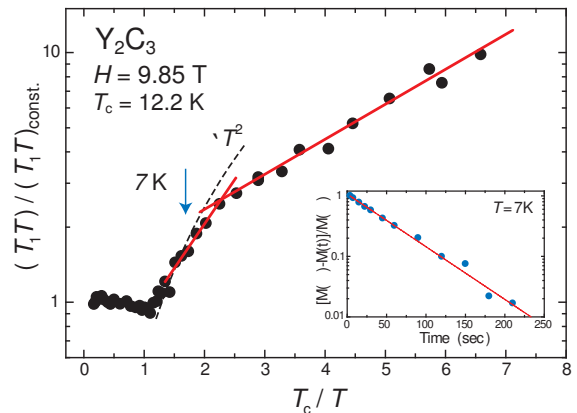


Fig. 4. (Color online) Arrhenius plot of  $(T_1T)/(T_1T)_{\text{const.}}$  vs  $T_c/T$  with  $T_c = 12.2\text{ K}$  at  $H = 9.85\text{ T}$ . From the respective slopes in the  $T$  range  $5\text{ K} - T_c = 12.2\text{ K}$  and at temperatures lower than  $5\text{ K}$ , gap sizes are estimated as  $2\Delta/k_B T_c \sim 5$  and  $2$ . The inset shows a simple exponential recovery curve of nuclear magnetization given by the relation  $[M(\infty) - M(t)]/M(\infty) = \exp(-t/T_1)$ . Here,  $M(t)$  and  $M(\infty)$  are the nuclear magnetizations at a time  $t$  after the saturation pulse and at the thermal equilibrium condition, respectively. Even in the SC state at  $T = 7\text{ K}$ , note that  $1/T_1$  for  $^{13}\text{C}$  with nuclear spin  $I = 1/2$  is uniquely determined (see the text).

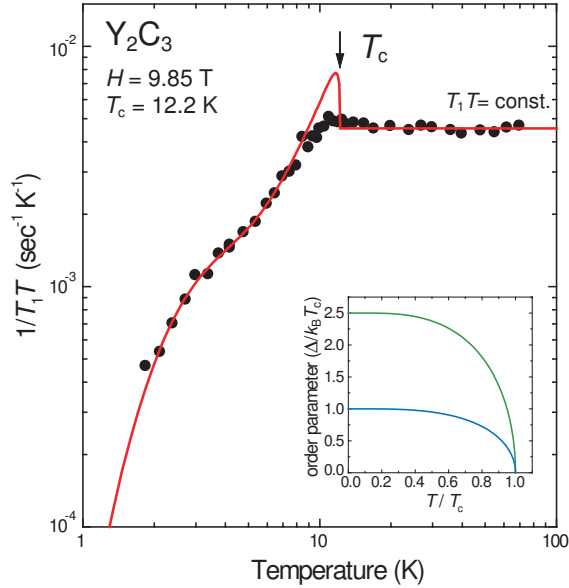


Fig. 5. (Color online)  $T$  dependence of  $1/T_1 T$  for  $\text{Y}_2\text{C}_3$  with  $T_c = 12.2\text{ K}$  at  $H = 9.85\text{ T}$ . A phenomenological multigap model for nodeless superconductivity is applied to understand the novel relaxation behavior in the SC state. The solid curve is a theoretical curve based on the multigap model with  $\beta = 0.75$  and  $2\Delta_\beta/k_B T_c = 5$  for the main band, and  $\alpha = 0.25$  and  $2\Delta_\alpha/k_B T_c = 2$  for other band (see the text). The inset shows the  $T$  dependences of the order parameters  $\Delta_\alpha$  and  $\Delta_\beta$ .

In conclusion, the superconducting properties of  $\text{Y}_2\text{C}_3$  with a relatively high transition temperature  $T_c = 15.7\text{ K}$  have been investigated using the  $^{13}\text{C}$  nuclear-magnetic-resonance (NMR) method under a magnetic field. The Knight shift has revealed a significant decrease below  $T_c$ , suggesting the spin-singlet superconductivity. The nuclear spin-lattice relaxation study in the SC state has revealed that  $\text{Y}_2\text{C}_3$  is a multigap superconductor that

exhibits a large gap  $2\Delta/k_B T_c = 5$  at the main band and a small gap  $2\Delta/k_B T_c = 2$  at others. These results have revealed that  $\text{Y}_2\text{C}_3$  is a unique multigap s-wave superconductor similar to  $\text{MgB}_2$ .

The authors would like to thank H. Kotegawa, M. Yogi, and H. Tou for fruitful discussions and comments, and N. Terasaki for experimental support. This work was supported by a Grant-in-Aid for Creative Scientific Research (15GS0213), MEXT and the 21st Century COE Program supported by the Japan Society for the Promotion of Science.

- 1) J. Nagamatsu, N. Nakagawa, T. Muranaka, Y. Zenitani, and J. Akimitsu: *Nature* **410** (2001) 63.
- 2) G. Amano, S. Akutagawa, T. Muranaka, Y. Zenitani, and J. Akimitsu: *J. Phys. Soc. Jpn.* **73** (2004) 530.
- 3) M. C. Krupka, A. L. Giorgi, N. H. Krikorian, and E. G. Szklarz: *J. Less-Common. Met.* **17** (1969) 91.
- 4) S. Akutagawa and J. Akimitsu: *J. Phys. Soc. Jpn.* **76** (2007) No2.
- 5) M. Yogi, Y. Kitaoka, S. Hashimoto, T. Yasuda, R. Settai, T. D. Matsuda, Y. Haga, Y. Onuki, P. Rogl, and E. Bauer: *Phys. Rev. Lett.* **93** (2004) 27003.
- 6) H. Q. Yuan, D. F. Agterberg, N. Hayashi, P. Badica, D. Vandervelde, K. Togano, M. Sigrist, and M. B. Salamon: *Phys. Rev. Lett.* **97** (2006) 017006.
- 7) P. G. De Gennes: *Superconductivity of Metals and Alloys*, translated by P. A. Pincus (W. A. Benjamin, New York, Amsterdam, 1966).
- 8) We use  $H_{c2} = -0.691(dH_{c2}/dT)T_c$  and  $\xi^2 = \phi_0/2\pi H_{c2}$  to get the value of  $\xi$ .  $d$  is estimated using  $d^2 = 2\phi_0/\sqrt{3}B$  (triangular lattice).  $\phi_0$  is the flux quantum.
- 9) D. J. Singh and I. I. Mazin: *Phys. Rev. B* **70** (2004) 052504.
- 10) H. Kotegawa, K. Ishida, Y. Kitaoka, T. Muranaka, and J. Akimitsu: *Phys. Rev. Lett.* **87** (2001) 127001.
- 11) S. Ohsugi, Y. Kitaoka, M. Kyogaku, K. Ishida, K. Asayama, and T. Ohtani: *J. Phys. Soc. Jpn.* **61** (1992) 3054.
- 12) L. C. Hebel and C. P. Slichter: *Phys. Rev.* **113** (1959) 1505.
- 13) L. C. Hebel and C. P. Slichter: *Phys. Rev.* **116** (1959) 79.